

# Liquid crystalline phases in DNA and dye-doped DNA solutions analysed by polarized linear and nonlinear microscopy and differential scanning calorimetry\*

J. OLESIAK<sup>1\*\*</sup>, K. MATCZYSZYN<sup>1</sup>, H. MOJZISOVA<sup>2</sup>,  
M. ZIELINSKI<sup>2</sup>, D. CHAUVAT<sup>2</sup>, J. ZYSS<sup>2</sup>

<sup>1</sup>Group of Physics and Chemistry of Molecular Materials, Institute of Physical and Theoretical Chemistry, Wrocław University of Technology, Wybrzeże Wyspiańskiego 27, 50-370 Wrocław, Poland

<sup>2</sup>Laboratoire de Photonique Quantique et Moléculaire, Ecole Normale Supérieure de Cachan, 61 avenue du Président Wilson, 94235 Cachan, Cedex, France

The contribution reports on an investigation of liquid crystalline phases in salmon (ca. 2000 bp) and herring (ca. 50 bp) roe DNA solutions in water. DNA aqueous solutions exhibit lyotropic liquid crystal (LLC) properties. To characterize LLC phases in DNA solutions, specially prepared LC cells as well as drying droplets were observed under a polarized light microscope (PLM). Differential scanning calorimetry (DSC) was used to determine the temperatures of phase transitions. The preliminary results are discussed and several structures of LLC in DNA aqueous solutions are presented as a function of temperature, concentration and DNA contour length. Apart from pure DNA solutions, a host-guest system was fabricated, with DNA doped with 4-(4-Nitrophenylazo)aniline – an azobenzene derivative, known as Disperse Orange 3 (DO3). In such a system, liquid crystalline phases were observed differing from the phases formed in pure DNA solutions of similar concentrations of matter. To study the mutual orientation of DNA chains and small dye molecules, polarization sensitive nonlinear microscopy was applied. DNA dissolved in water and doped with azobenzene was found to produce a two-photon fluorescence signal. From polarization analysis, a partial ordering of DO3 molecules in DNA matrix was observed.

Key words: *DNA liquid crystal phases; calorimetry; polarized light microscopy; Disperse Orange 3; two photon fluorescence; nonlinear polarimetry analysis*

## 1. Introduction

The very first observations of liquid crystalline phases in DNA solutions in water or buffers were described in the 1950s [1]. It was assumed that ordering of DNA

---

\*The paper presented at the 11th International Conference on Electrical and Related Properties of Organic Solids (ERPOS-11), July 13–17, 2008, Piechowice, Poland.

\*\*Corresponding author, e-mail: joanna.olesiak@pwr.wroc.pl

chains has a profound impact on their function as well as their configuration in a cellular environment. The following decades brought new data on the lyotropic liquid crystalline (LLC) phases in DNA aqueous solutions. The relation between the creation of LLC and numerous parameters was investigated: dependence on temperature, DNA concentration, ionic strength of a solution and occurring counterions [2]. The features of the double helix, i.e. its length, topology, the sequence of bases, were also found to influence the observed phases [3, 4].

A number of fluorescent dyes and NLO chromophores can be doped to DNA matrix. They can intercalate into a DNA helix, bind to DNA grooves or just weakly interact with double strands in a solution. Mutual interactions affect optical properties of dyes and increase photoluminescence intensity, which has robust applications. It is commonly used to stain DNA for microscopy, and is exploited in diverse methods of gel-based nucleic acid separation, with the use of ethidium bromide, acridine orange or Hoechst stain [5]. It can also be applied to the detection of mismatched sites in double-stranded DNA, with the use of destabilizing agents, e.g. octahedral rhodium(III) complexes [6]. Furthermore, it is applied to sensing in DNA microarrays [7] as well as biosensor devices.

DNA modified with a cationic surfactant and doped with photoactive dyes is a promising material for applications in photonics because of its exceptional structure and excellent optical properties [8, 9]. Azobenzenes are suitable dopants for DNA-based photoactive materials, as their optical and photochemical properties are well known and widely applied in combination with liquid crystals [10–13]. To date, only a few studies have been reported on azobenzene–DNA interactions [14] and the nature of binding is still in debate.

We propose to apply linear and nonlinear microscopy as well as differential scanning calorimetry to investigate arrangements of azobenzene molecules and DNA. More specifically, we observe polymorphism of DNA configuration in order to find the specific range of temperature and concentration where individual phases exist. We characterize DNA matrix doped with 4-(4-nitrophenylazo)aniline (Disperse Orange 3) by polarized light microscopy and differential scanning calorimetry and compare to pure DNA solutions. Then, nonlinear microscopy allows us to extract further information about the mutual orientation of long chains of DNA and the molecules of the dopant.

## 2. Materials and methods

*Sample preparation.* Marine-based DNA isolated from salmon and herring roe was purchased from Sigma-Aldrich. According to the information provided by the supplier, salmon DNA contains approximately 2000 base pairs (bp), with MW around  $1.3 \times 10^6$ . The melting temperature ( $T_m$ ) is about 87.5 °C. To confirm the exact size of strands, electrophoresis was performed in agarose gel (70 V and 0.5 A,  $t = 20$  min). Lambda DNA/PstI Marker was used, which covers the range 15–11501 bp. Visualized

fringes of salmon DNA spread as one smear from 260 bp (very low intensity) to ca. 6000 bp. The purity of DNA was confirmed, the results indicate, however, that the length of individual chains are distributed over a very broad range. Herring DNA oligonucleotides are 50 bp long.

4-(4-Nitrophenylazo)aniline, an azobenzene derivative known as Disperse Orange 3 (DO3), was bought from Sigma-Aldrich. According to the information sheet provided, the absorbance maximum of the *trans* form is at 443 nm. Absorption spectra of DNA, DO3 and DNA doped with DO3 were recorded and the maxima of absorption were established. For pure DNA (concentration ca. 0.2 mg/cm<sup>3</sup>)  $\lambda_{\text{max}} = 260$  nm, for DO3 aqueous solution  $\lambda_{\text{max}} = 403$  nm. Absorption spectra of DNA and DO3 solutions in water show two separate maxima, one related to DNA absorption and the other one, around  $\lambda_{\text{max}}$  of DO3. The presence of the latter one is an indication that this particular dye does not intercalate into the DNA chains (Fig. 1).

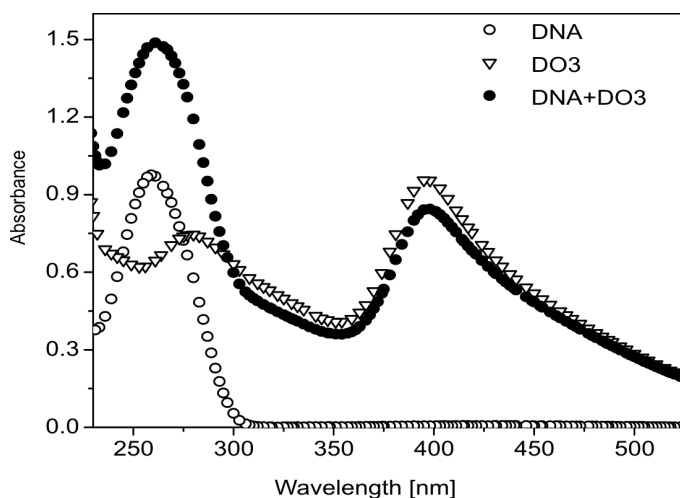


Fig. 1. Absorption spectra of pure DNA solution, DO3 solution and DNA-DO3 solution

*Polarized light microscopy (PLM).* Prior to PLM analysis, both salmon and herring DNA were dissolved in water and sodium salt solutions were obtained in a concentration range from  $c_{\text{DNA}} = 3$  mg/cm<sup>3</sup> to 120 mg/cm<sup>3</sup>. DO3 aqueous solutions were obtained after several hours of sonication, followed by filtration. DNA solutions and DNA solutions doped with DO3 were deposited atop glass plates and several kinds of samples were prepared: droplets of the volume 5–15  $\mu\text{l}$  and cells built of two glass plates with Teflon spacers of the thickness of 6  $\mu\text{m}$ , 70  $\mu\text{m}$  and 1 mm. PLM photographs were taken under an Olympus 60BX microscope equipped with a hot stage, under a crossed polarizer condition.

*Differential scanning calorimetry (DSC).* DSC measurements were performed with a Perkin Elmer DSC7 at a scan rate of 1 or 2  $^{\circ}\text{C}/\text{min}$ . Each sample was heated from the room temperature to almost 100  $^{\circ}\text{C}$  and then cooled down to 25  $^{\circ}\text{C}$ .

*Two photon fluorescence (TPF) microscopy.* Nonlinear optical properties of DNA and DO3 were investigated by nonlinear microscopy combined with polarimetric detection [15]. The source of light was a Ti:Sa laser (100 fs, 80 MHz repetition rate) with the incident wavelength in the range 680–1020 nm. The laser beam, after passing through a Glan–Taylor prism polarizer, passed through an achromatic half-wave plate mounted on a motorized rotation stage, in order to continuously vary the polarization direction of the incident light. Then the beam was focused on the sample through a high numerical aperture oil immersion objective ( $\times 100$ ,  $NA = 1.4$ ). The sample was mounted on an  $xyz$  piezoelectric scanning system which was moved in its plane with a scan step of 20 nm or greater. The spot size was about 350 nm. The TPF emission was collected in epifluorescence mode through the same high numerical aperture objective and split by a polarizing beam splitter. That resulted in orthogonally polarized signals, which were recorded by two avalanche photodiodes operating in the photon counting regime.

### 3. Results and discussion

DNA strands in aqueous solutions exhibit wide polymorphism and lyotropic liquid crystalline (LLC) properties. To establish a critical concentration required to create LLC phases, solutions of salmon and herring DNA were prepared and observed as droplets under PLM. The first anisotropic phase in salmon DNA samples appeared for  $c_{\text{DNA}} < 3 \text{ mg/cm}^3$ .

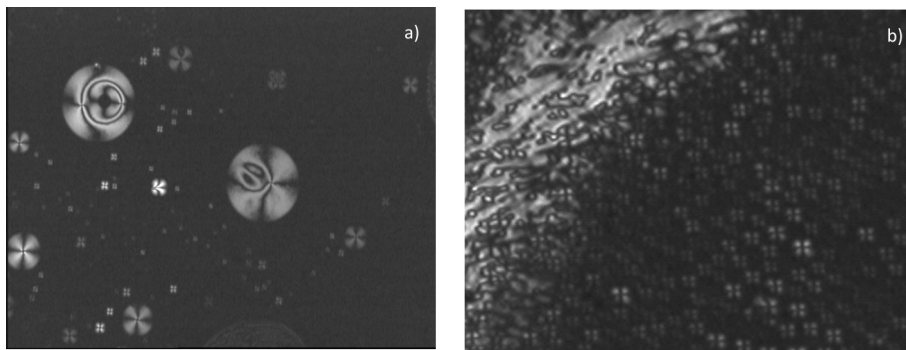


Fig. 2. Nematic extinction brushes in salmon DNA solution (a),  $c_{\text{DNA}} < 3 \text{ mg/cm}^3$  and LLC phases in herring DNA solution (b),  $c_{\text{DNA}} = 70 \text{ mg/cm}^3$

In these conditions, Schlieren textures, characteristic of nematics, were observed, as is shown in Fig. 2a. The critical concentration required to form LLC phases in shorter, herring DNA strands was significantly higher. In this case, LLC lamellar phases were obtained in aqueous solutions with  $c_{\text{DNA}} > 70 \text{ mg/cm}^3$  (Fig. 2 b). After these preliminary results with herring DNA, all the subsequent experiments were conducted with salmon DNA solutions. In the following paragraphs, we describe the most

characteristic phases observed in specific ranges of salmon DNA concentration and temperature, for both, pure and dye-doped DNA.

### 3.1. Drying droplets

In drying droplets of DNA solution with low concentration of DNA ( $10 \text{ mg/cm}^3 < c_{\text{DNA}} < 20 \text{ mg/cm}^3$ ) characteristic zig-zag forms are created, described previously by Smalyukh et al. [16] (Fig. 3a). They result from competition between the radial stress

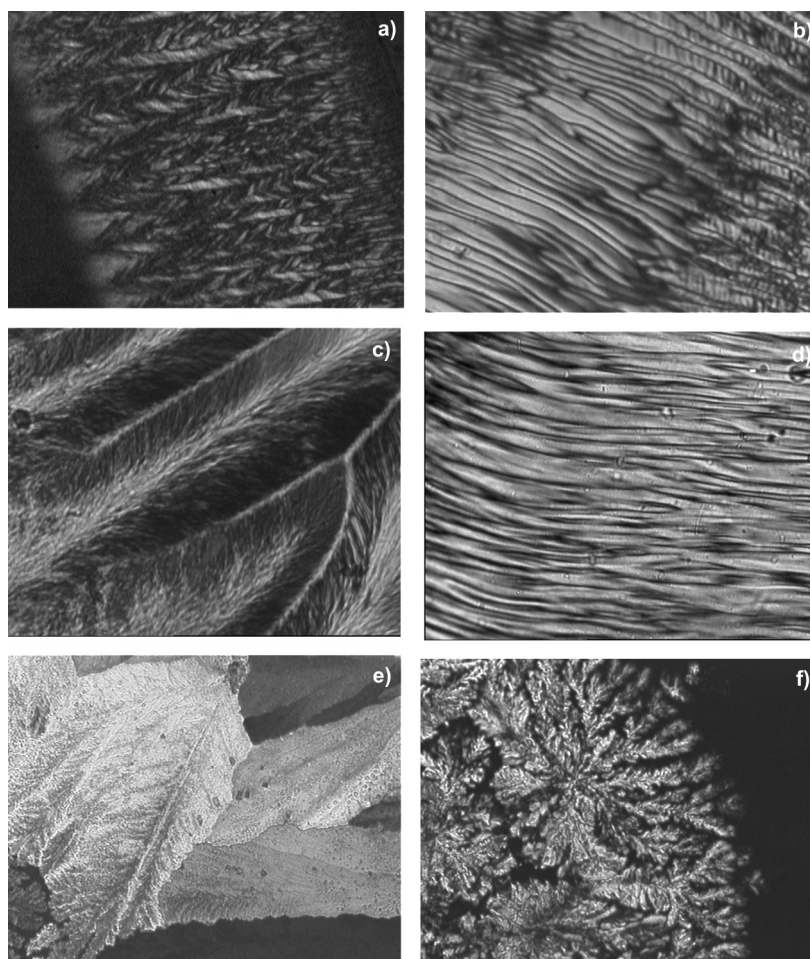


Fig. 3. Zig-zag pattern in drying droplet of DNA solution,  $c_{\text{DNA}} = 13 \text{ mg/cm}^3$ ,  $h = 176 \mu\text{m}$  (a), columnar structure in DNA drying droplet,  $c_{\text{DNA}} = 27 \text{ mg/cm}^3$ ,  $h = 157 \mu\text{m}$  (b), undulating columnar phase in DNA-DO3 drying droplet,  $c_{\text{DNA}} = 15 \text{ mg/cm}^3$ ,  $h = 90 \mu\text{m}$  (c), striped texture in drying DNA-DO3 droplet,  $c_{\text{DNA}} = 20 \text{ mg/cm}^3$ ,  $h = 235 \mu\text{m}$  (d), and centres of a droplet of DNA-DO3 solution with  $c_{\text{DNA}} = 10 \text{ mg/cm}^3$  (e) and  $c_{\text{DNA}} = 15 \text{ mg/cm}^3$  (f), respectively,  $h = 235 \mu\text{m}$ ,  $h$  is the overall height of the image

tending to stretch DNA strands along the radius of a droplet, and the LC elasticity that aligns DNA parallel to the contact line. For higher DNA concentrations ( $c_{\text{DNA}} > 20 \text{ mg/cm}^3$ ) a kind of columnar phase is created, shown in Fig. 3b.

A similar behaviour is observed in DNA-DO3 drying droplets ( $10 \text{ mg/cm}^3 < c_{\text{DNA}} < 18 \text{ mg/cm}^3$ ). PLM images present several zones, with the zig-zag texture nearby the contact line, followed by undulating columnar hexagonal phase (Fig. 3c). However, in the centre of the droplet, dendrimeric phases are formed, not observed in pure DNA solutions (Figs. 3e, f). This spatial distribution of phases can be related to the dispersion of DNA lengths as well as the process of migration of DNA strands. Some portion of DNA molecules accumulate by the contact line of a droplet and form the outermost thick ring. The remaining DNA chains are deposited as the inner rings, and are separated by the black areas which presumably consist of cholesteric phases. The mechanism of dendrimeric phase formation in DNA-DO3 droplets is under investigation. In DNA-DO3 solutions with  $c_{\text{DNA}} > 20 \text{ mg/cm}^3$ , a striped pattern is observed, as shown in Fig. 3d. It can be related to the columnar phase observed in pure DNA solution.

### 3.2. LC cells

LC cells were prepared with concentrated solutions of DNA and DNA-DO3. For  $c_{\text{DNA}} = 15 \text{ mg/cm}^3$  birefringent phases were hardly visible, as the evaporation of a solvent was constricted by the cover glass and the spacer. For  $c_{\text{DNA}} = 30 \text{ mg/cm}^3$  and  $60 \text{ mg/cm}^3$ , cholesteric liquid crystals were obtained for both, pure and doped DNA.

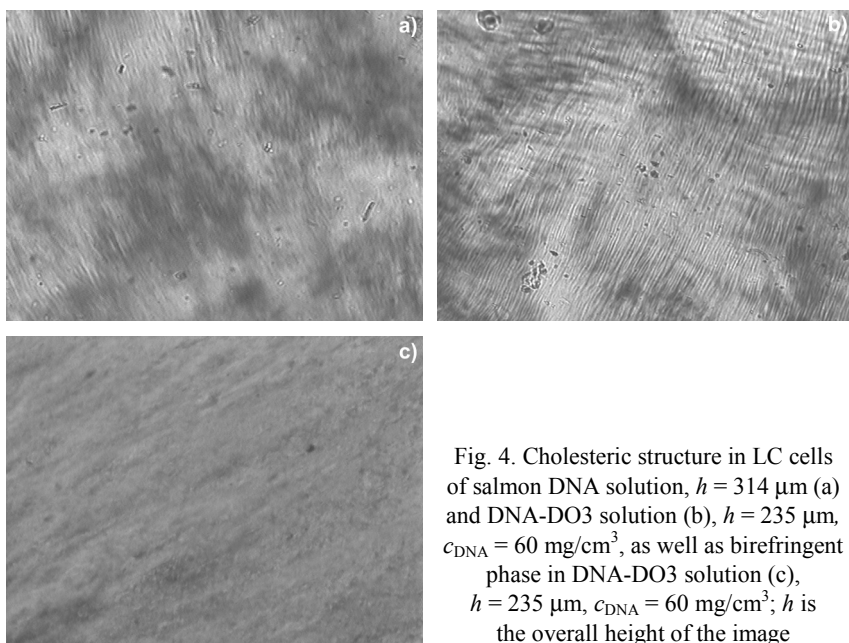


Fig. 4. Cholesteric structure in LC cells of salmon DNA solution,  $h = 314 \mu\text{m}$  (a) and DNA-DO3 solution (b),  $h = 235 \mu\text{m}$ ,  $c_{\text{DNA}} = 60 \text{ mg/cm}^3$ , as well as birefringent phase in DNA-DO3 solution (c),  $h = 235 \mu\text{m}$ ,  $c_{\text{DNA}} = 60 \text{ mg/cm}^3$ ;  $h$  is the overall height of the image

Figure 4 presents their characteristic fingerprint patterns. However, in some concentrated samples, domains of birefringent phase could be observed without stripes specific of cholesteric phase. We assume that they are related to DNA molecules unidirectionally aligned, otherwise without any higher ordering or rotation between the planes in which the molecules are aligned (Fig. 4c).

Pure DNA and DNA-DO3 solutions, observed in heated LC cells under PLM, exhibit two main transitions. Considering pure DNA, the first, less profound transition is observed at 66–70 °C. At ca. 84 °C, a black image corresponding to the order-disorder phase transition begins to appear. The uniformly black area, indicating an isotropic solution, is obtained at 86 °C. In the case of DNA doped with DO3, the cholesteric pattern of DNA-DO3 solution vanishes at 50–53 °C, and a plain, birefringent phase is observed. The order-disorder transition starts at ~58 °C and ends at ~68 °C. Both processes are reversible and a clearly visible, birefringent area appears upon cooling.

### 3.3. DSC measurements

DSC runs were carried out in the same temperature range just as for the PLM images (from 25 °C to 100 °C) for several samples with various concentrations of salmon DNA. Relative changes in the heat flow were very small and difficult to observe in more diluted solutions ( $c_{\text{DNA}} < 30 \text{ mg/cm}^3$ ). The positions of the peaks evaluated with the use of DSC software are presented in Table 1.

Table 1. DSC peaks positions in salmon DNA samples of various concentrations, pure or doped with DO3 molecules

Solution	dry DNA	120 mg/cm <sup>3</sup> DNA	60 mg/cm <sup>3</sup> DNA	30 mg/cm <sup>3</sup> DNA	15 mg/cm <sup>3</sup> DNA
DNA	92.85 °C	75.78 °C	74.77 °C 93.10 °C	70.44 °C 93.08 °C	poorly resolved peak ca. 73 °C
DNA + DO3	—	—	71.28 °C 93.12 °C	70.53 °C 93.11 °C	poorly resolved peak ca. 77 °C

Analysing DSC plots, we can distinguish two main processes; one around 70–75 °C and the other at 93 °C (Fig. 5a).  $T_m = 93 \text{ °C}$  is the melting temperature of DNA strands, which is confirmed by DSC measurement in dry DNA. Denaturation does not depend on DNA concentration. However, a temperature shift is observed for a DNA-DO3 system, as plotted in Fig. 5b. DO3 molecules may destabilize DNA chains, thereby resulting in a lower denaturation temperature and the occurrence of an order-disorder transition already at ca. 68 °C. The other, broad peak corresponds to a change in the cholesteric structure, similar to the transition observed by Kagemoto et al. at 70 °C [17]. Differences in temperature evaluated from DSC and PLM observations may exist due to different conditions of sample preparation and investigation.

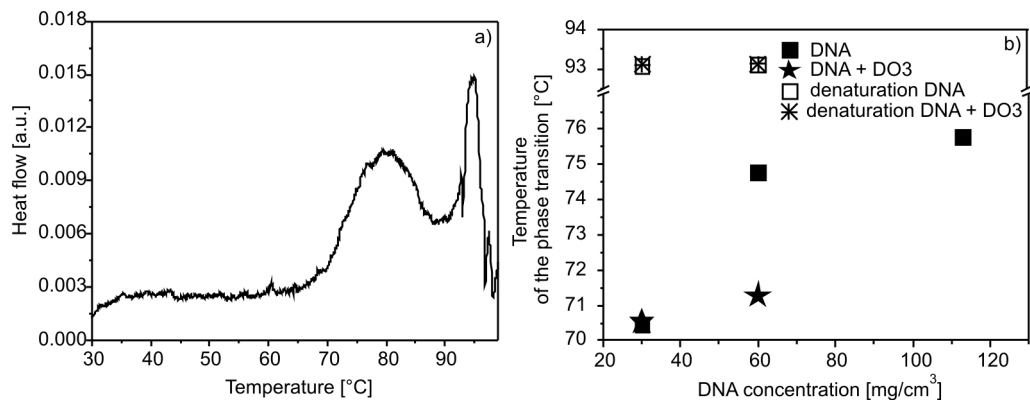


Fig. 5. DSC plot of DNA solution doped with DO3,  $c_{\text{DNA}} = 60 \text{ mg/cm}^3$  (a) and the dependence of temperatures of two main phase transitions in pure DNA and doped DNA solutions on the DNA concentration (b)

Material sealed in DSC vessels is isolated from the environment, thus drying, evaporation of a solvent and non-uniform heating in the cell volume do not affect the measurement.

### 3.4. Nonlinear polarimetry analysis

Since the absorption and the fluorescence emission processes are sensitive to the polarization of the excitation light, nonlinear optical polarimetry was considered to be a valuable technique to determine the local ordering of sample molecules [15, 18, 19]. If a solution of randomly oriented absorbing molecules is irradiated with polarized light, the average absorption is independent of the incident polarization. However, if the absorbing molecules are at least partly oriented, the absorption will occur preferentially along the polarization direction parallel to the absorbing transition dipoles. Similarly, the fluorescence emission occurs in a clearly identifiable axis, parallel to the axis of the emission dipole of the ordered molecules. Therefore, detection of fluorescence intensity at various incident polarizations allows us to determine the orientation of emission dipoles projection in a macroscopic  $XY$  coordinate system.

DO3 is a rod-like molecule with a central conjugated system and a couple of electron donor and acceptor groups on the extremities. In a rough approximation, it was assumed that the absorption and emission dipoles are parallel to the long molecular axis.

As a first attempt to apply the nonlinear microscopy to dye-doped DNA liquid crystal we chose one of the above mentioned sample configurations, i.e., DNA-DO3 in a closed cell with  $c_{\text{DNA}} = 60 \text{ mg/cm}^3$ . The structure of the sample is presented in Fig. 4c.

DO3 molecules were excited at 810 nm, equivalent to 405 nm for one photon excitation, and the emitted fluorescence was recorded in the spectral range between 400 nm and 650 nm. The maximum light intensity incident on the sample was



800  $\mu\text{W}$ . In these experimental conditions, the intrinsic DNA two-photon fluorescence signal is found to be negligible compared with the DO3 emission.

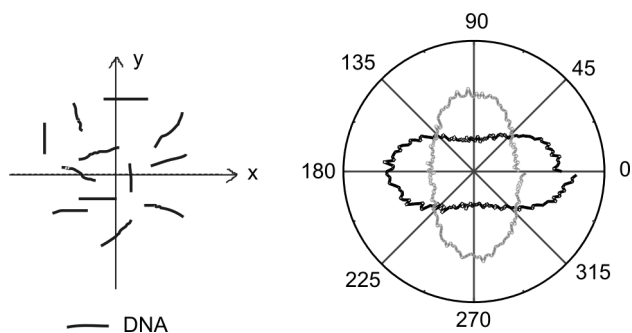


Fig. 6. Polar graphs of the isotropic solution of DNA-DO3

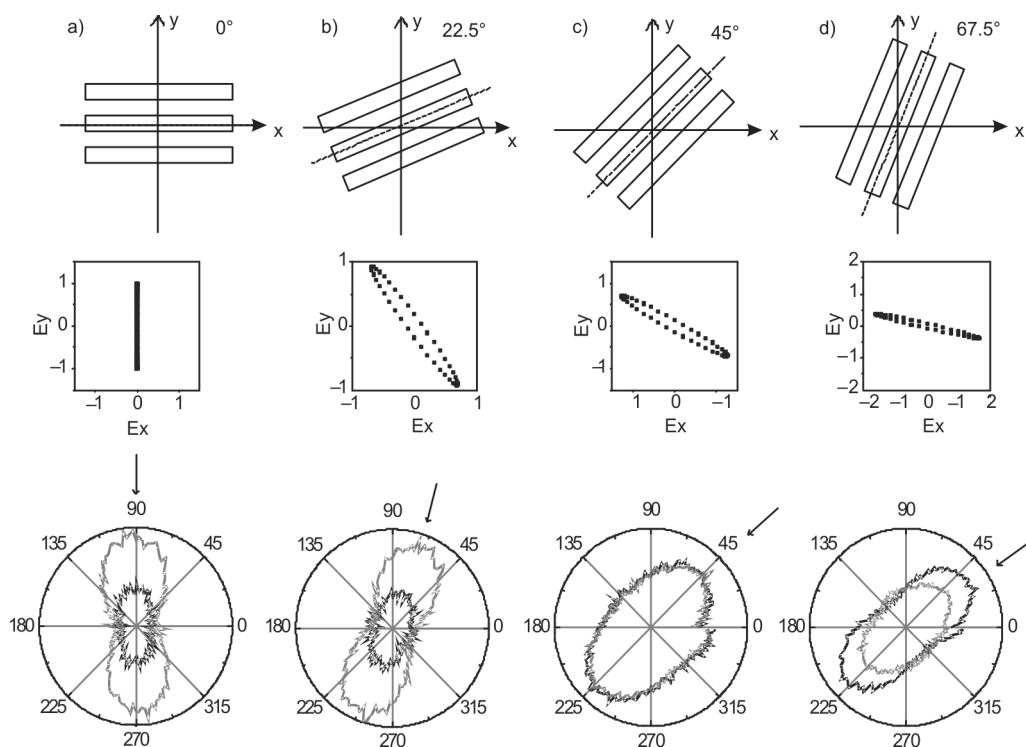


Fig. 7. Rotation of the sample in the  $XY$  framework: 1st row: scheme of the orientation of DNA domains. The dashed line represents the long axis of the domain. 2nd row: theoretical modelling of the deformation of the incident linear polarization at angles corresponding to the maximum TPF intensity for every polar graph (denoted by arrows). 3rd row: polar graphs of TPF emitted by DO3 in a DNA liquid crystal

First, we consider a reference sample where DNA-DO3 solution is isotropic liquid phase. Figure 6 shows typical polar graphs of fluorescence intensity of  $X$  and  $Y$  polari-

zation components emitted by DO3. The crossed pattern indicates a random orientation of the emitting dipoles. Conversely, Figure 7a represents polar graphs recorded in samples where DNA has an ordered distribution in liquid crystal domains. The two  $X$  and  $Y$  components are aligned parallel to each other and their orientation refers to the orientation of DO3 linked to DNA strands. Clearly, the alignment of DO3 molecules appears to be perpendicular to the alignment of the DNA strands. In order to confirm that this orientation is imposed by DNA strands, and to avoid any light-induced alignment of DO3 molecules, the sample was rotated in the  $XY$  plane and the polarimetric measurements were taken at a few different positions. The orientation of liquid crystalline texture and the corresponding polar graphs are shown in Figs. 7b–d.

Care has to be taken in analysis of a few data, since the actual light polarization on the sample depends on some optical parameters of the setup such as the birefringence of the optical elements and namely of the dichroic mirror. More specifically, the incident polarization is shown in Fig. 7. If we consider the angle of the maximum fluorescence intensity, we observe that it corresponds to an elliptic incident polarization, which is roughly oriented at  $90^\circ$  to the DNA texture. Therefore this sample rotation and corresponding analysis confirm the orientation of DO3 at about  $90^\circ$  relative to the DNA LC pattern. A more detailed mathematical analysis will be published elsewhere.

## 4. Conclusions

DNA dissolved in water forms lyotropic liquid crystalline phases (nematic, cholesteric, columnar) depending on DNA length, concentration and temperature, which were observed by polarized light microscopy. Similar liquid crystalline phases are created in LC cells filled with DNA solutions doped with 4-(4-Nitrophenylazo)aniline (DO3). However, phase transitions in the DNA-DO3 system occur at temperatures lower than those in pure DNA solutions. Moreover, in drying droplets of DNA-DO3 additional dendrimeric phases appear in the centre of a droplet, apart from the zig-zag pattern and columnar phases observed at the rim of the droplet in both, pure DNA and DNA-DO3 solutions. According to nonlinear polarimetry analysis, DO3 is oriented by DNA strands. The relative angle between liquid crystalline textures of DNA and the long axis of the DO3 molecule is approximately  $90^\circ$ . Nonlinear polarimetry thus appears as a useful tool to analyze the relative orientation of a dye and DNA molecules, and could be applied locally to understand, for instance, the additional dendrimeric and columnar phases found in dye-doped DNA solutions. This work is currently in progress in our laboratory.

## Acknowledgements

This work was supported by the European Commission through the Human Potential Programme (Marie-Curie RTN BIMORE, Grant No. MRTN-CT-2006-035859), grant no. N50713231/3302 and IMFOVIR Project ANR-06-PCVI-0015 as well as through the Wrocław University of Technology. We express our gratitude to Prof. Juliusz Sworakowski for helpful discussions.

## References

- [1] LUZZATI V., NICOLAIEFF A., *J. Mol. Biol.*, 1 (1959), 127.
- [2] LIVOLANT F., LEFORESTIER A., *Prog. Polym. Sci.*, 21 (1996), 1115.
- [3] KASSAPIDOU K., JESSE W., VAN DIJK J.A.P.P., VAN DER MAAREL J.R.C., *Biopolymers*, 46 (1998), 31.
- [4] MERCHANT K., RILL R.L., *Biophys. J.*, 73 (1997), 3154.
- [5] LI Y., DICK W.A., TUOVINEN O.H., *Biol. Fertil. Soils*, 39 (2004), 301.
- [6] JUNICKE H., HART J.R., KISKO J., GLEBOV O., KIRSCH I.R., BARTON J.K., *Proc. Natl Acad. Sci. USA*, 100 (2003), 3737.
- [7] LEE N.H., SAEED A.I., *Methods Mol. Biol.*, 353 (2007), 265.
- [8] HE G.S., ZHENG Q., PRASAD P.N., GROTE J.G., HOPKINS F.K., *Opt. Lett.*, 31 (2006), 359.
- [9] GROTE J.G., DIGGS D.E., NELSON R.L., ZETTS J.S., HOPKINS F.K., OGATA N., HAGEN J.A., HECKMAN E., YANEY P.P., STONE M.O., DALTON L.R., *Mol. Cryst. Liq. Cryst.*, 426 (2005), 3.
- [10] NATANSOHN A., ROCHON P., *Chem. Rev.*, 102 (2002) 4139.
- [11] YESODHA S.K., SADASHIVA PILLAI C.K., TSUTSUMI N., *Prog. Polym. Sci.*, 29 (2004), 45.
- [12] MATCZYSZYN K., SWORAKOWSKI J., *J. Phys. Chem. B*, 107 (2003), 6039.
- [13] MATCZYSZYN K., CHWIAKOWSKA A., SWORAKOWSKI J., *Thin Solid Films*, 516 (2008), 8899.
- [14] SNYDER R.D., MCNULTY J., ZAIROV G., EWING D.E., HENDRY L.B., *Mut. Res.*, 578 (2005), 88.
- [15] BRASSELET S., LE FLOC'H V., TREUSSART F., ROCH J.-F., ZYSS J., BOTZUNG-APPERT E., IBANEZ A., *Phys. Rev. Lett.*, 92 (2004), 207401.
- [16] SMALYUKH I., ZRIBI O.V., BUTLER J.C., LAVRENTOVICH J.D., WONG G.C.L., *Phys. Rev. Lett.*, 96 (2006), 177801-1.
- [17] KAGEMOTO A., NAKAZAKI M., KIMURA S., MOMOHARA Y., UENO K., BABA Y., *Thermochim. Acta*, 284 (1996), 309.
- [18] LE FLOC'H V., BRASSELET S., ROCH J.-F., ZYSS J., *J. Phys. Chem. B*, 107 (2003), 12403.
- [19] BRASSELET S., ZYSS J., *Compt. Rend. Phys.*, 8 (2007), 165.

*Received 26 October 2008*

*Revised 8 January 2009*